Structural and Soft Hysteresis loops of Mg-Cu-Sm nano ferrites by Citrate gel method

G. Satyanarayana Goud [1*] , R. Gangadhara[2], Shankar Barapati[3], P Veerasomaiah[4]

1 Department of Chemistry, MVS Govt. Arts and Science College, Mahabubnagar, Telangana, India.509001.
2 Department of Chemistry, Stanley College of Engineering & Technology for Women, Hyderabad, India.500 001
3 Department of Humanities and Sciences, JNTUH University College of Engineering, Manthani, Telangana India.505212.
4 Department of Chemistry, University college of science, Osmania University, Hyderabad, Telangana, India 500 007
***Author for correspondence Email:** gangarigoud@gmail.com

Abstract

$Mg_{0.5}Cu_{0.5}Sm_{0.25}Fe_{1.75}O_4$ nano ferrite were synthesized using the citrate gel auto combustion technique and then calcined at 500°C. The resulting sample's optical, magnetic, and structural characteristics were examined. X-ray diffraction (XRD), Fourier-transform infrared spectroscopy (FTIR), and Raman spectroscopy were used to analyse the structural characteristics. A single-phase cubic spinel structure with a crystalline size of 8.69 nm was confirmed to have formed by XRD analysis. FTIR spectra were used to confirm that the composition contained tetrahedral and octahedral sites. The Raman spectrum showed the distinctive A_{1g}, E_g, and $3T_{2g}$ modes that group theory predicted. A saturation magnetization of 27.78 emu/gm was discovered through analysis using a vibrating sample magnetometer (VSM) at room temperature.

Keywords: *$Mg_{0.5}Cu_{0.5}Sm_{0.25}Fe_{1.75}O_4$ nano ferrite, citrate-gel method, structural properties, hysteresis loops.*

1. Introduction

Iron oxide (Fe_2O_3) mostly combines with divalent or trivalent metal oxides like Mg-O, Ni-O, Mn-O, Cu-O, or Cr-O to form ceramic ferrites, a class of magnetic materials. Because of their high resistivity, low eddy current losses, and good chemical stability, these polycrystalline ceramics which display ferrimagnetic behaviour find extensive use in electronic, magnetic, and microwave applications[1,2] Ferrites are typically produced as fine, homogenous nanoparticles with regulated stoichiometry and morphology using ceramic, sol-gel, or citrate-gel auto-combustion techniques. Ferrites form crystals in a spinel pattern. This structure follows the formula MFe_2O_4. Here, M stands for a metal ion with two positive charges. Common choices include nickel (Ni^{2+}), cadmium (Cd^{2+}), cobalt (Co^{2+}), or zinc (Zn^{2+}). These materials play key roles in magnets and electronics. They help store data or filter signals in devices like hard drives and antennas[3,4]. The setup starts with oxygen ions packed tight in a cubic form. This close pack leaves gaps for metal ions. Two main gap types exist: tetrahedral sites and octahedral sites. Tetrahedral sites look like a four-sided shape with the ion at the centre. Octahedral sites have six sides around the ion. This arrangement gives ferrites their strength and unique traits[5–7]. In normal spinel ferrites, the divalent metal ions fill the tetrahedral sites. All the iron ions (Fe^{3+}) take the octahedral sites. Take magnesium ferrite as an example. It shows this normal setup well. Such ferrites often have steady magnetic pull that resists change. Inverse spinel ferrites shift things around. Here, iron ions split evenly between tetrahedral and octahedral sites[8,9]. The divalent metals claim the leftover octahedral spots. Magnetite, or Fe_3O_4, fits this inverse type. It forms from iron oxide and powers

many magnetic tools. In the present study, $Mg_{0.5}Cu_{0.5}Sm_{0.25}Fe_{1.75}O_4$ was synthesized by the citrate-gel auto-combustion method, and its structural characterization like XRD, FTIR, Raman as well as magnetic properties were investigated.

2. Experimental methods

2.1 Preparation of sample

The $Mg_{0.5}Cu_{0.5}Sm_{0.25}Fe_{1.75}O_4$ nanoferrite was successfully synthesized using the versatile and widely applied citrate-gel auto-combustion method, which is preferred for its ability to produce highly crystalline and homogeneous nano powders. The process begins with the careful preparation of an aqueous precursor solution. Stoichiometric amounts of the required metal nitrates specifically magnesium nitrate, copper nitrate, samarium nitrate and ferric nitrate are accurately weighed to achieve the final composition and subsequently dissolved completely in a minimal volume of distilled water to form a clear solution. The crucial step involves the addition of citric acid and EDTA (ethylenediaminetetraacetic acid) in specific molar ratios, serving as chelating agents or fuels. These agents effectively complex with the metal ions, preventing premature precipitation and ensuring that the cations are distributed uniformly at the atomic level throughout the solution, a key factor for the final product's homogeneity[10,11]. The resulting solution is then heated, typically on a hot plate with continuous stirring, to promote water evaporation and initiate gel formation. As the temperature increases and the water is driven off, the viscous gel spontaneously ignites due to the highly exothermic redox reaction between the metal nitrates (oxidizers) and the citric acid/EDTA (fuel/reducers). This rapid, self-propagating combustion rapidly converts the mixture into a loose, fluffy, voluminous ash which consists of the as-synthesized nanoferrite material, often requiring a final, brief thermal treatment or calcination (500^{O}C) to achieve the desired phase purity and optimal crystallite size. Fig.1 shows the flow chart for synthesis of $Mg_{0.5}Cu_{0.5}Sm_{0.25}Fe_{1.75}O_4$ nano ferrites

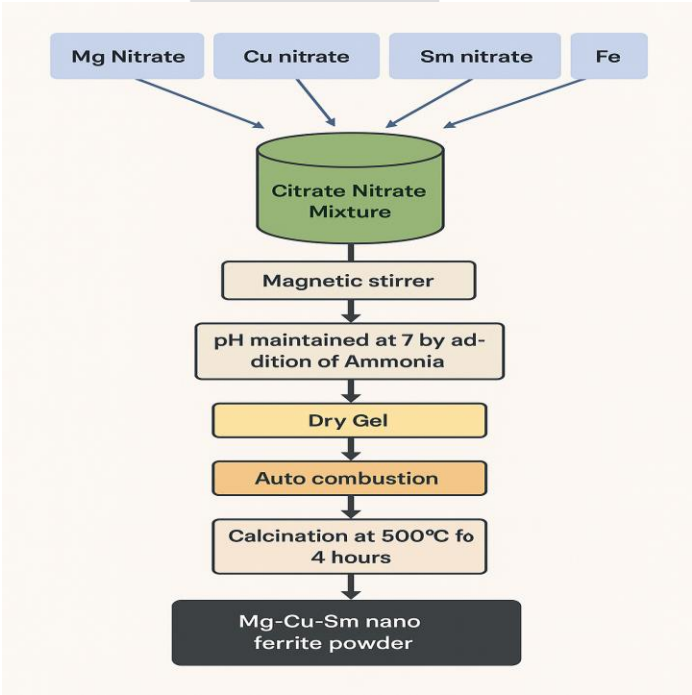

Fig.1 Synthesis of $Mg_{0.5}Cu_{0.5}Sm_{0.25}Fe_{1.75}O_4$ nano ferrites

3. Results and discussions

3.1 XRD

One of the most important methods for figuring out the structural characteristics of crystalline materials, such ferrites, is X-ray diffraction (XRD) analysis. It offers comprehensive details on the average crystallite size, lattice characteristics, phase development, and crystal structure of produced nanoparticles[12,13]. The creation of a single-phase spinel structure in $Mg_{0.5}Cu_{0.5}Sm_{0.25}Fe_{1.75}O_4$ nano ferrites made using the citrate-gel auto-combustion process was verified in the current study using XRD analysis shown in **Fig.2**. Good crystallinity of the produced sample was indicated by the strong and distinct diffraction peaks found in the XRD pattern. The (220), (311), (400), (422), (511), and (440) planes the distinctive reflections of a cubic spinel ferrite structure correspond to the measured diffraction peaks[14,15]. The dominating spinel phase development was confirmed by the observation of the most extreme peak at the (311) plane. The effective synthesis of $Mg_{0.5}Cu_{0.5}Sm_{0.25}Fe_{1.75}O_4$ ferrite without any impurity phases was confirmed by the peak positions and their accompanying Miller indices[16].

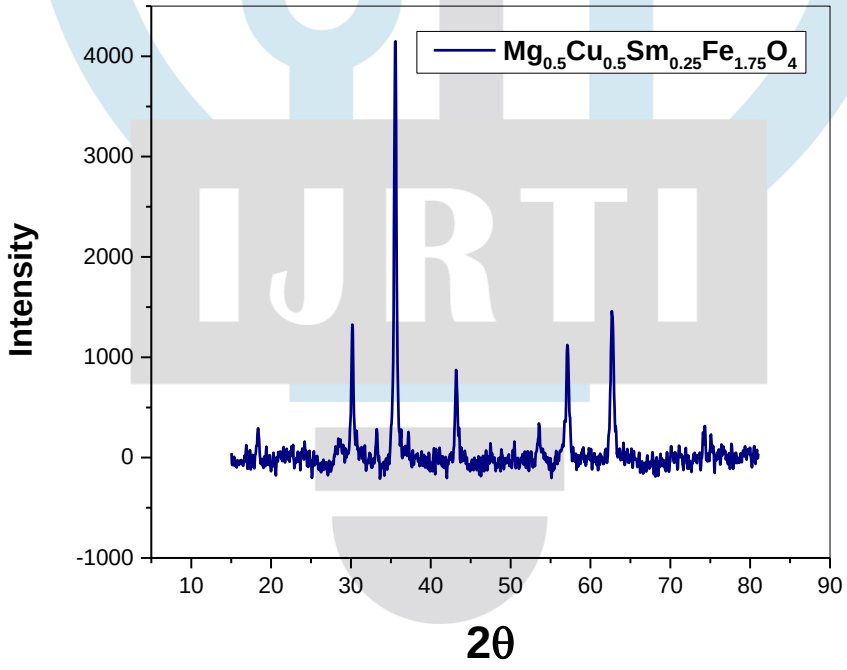

Fig.2 X-ray diffraction pattern of $Mg_{0.5}Cu_{0.5}Sm_{0.25}Fe_{1.75}O_4$ nano ferrites

Using the Debye-Scherrer formula, D=0.94λ/βCOṢ, where (λ) is the X-ray wavelength, (β) is the full width at half maximum (FWHM) of the peak, and (θ) is the Bragg's angle, the average crystallite size (D) of the $Mg_{0.5}Cu_{0.5}Sm_{0.25}Fe_{1.75}O_4$ nanoparticles was determined. The material is in the nanometer range, as indicated by the predicted crystallite size of 28.69 nm, Using Bragg's law and the formula. $a = d\sqrt{h^2 + k^2} + l^2$, the lattice parameter (a) of the cubic spinel structure was determined to be 7.89 Å. This result validates the correct substitution of Mg^{2+} ions in the Cu^{2+} lattice positions and is in good agreement with values reported for similar Mg-Ci-Sm nano ferrite systems[17,18]. Using the formula $V=a^3$, the unit cell volume (V) was calculated and came out to be roughly 491.169 Å, which is in line with the cubic spinel structure. Using the formula, the X-ray density (Dx) was determined. $Dx=\frac{8M}{N_A a^3}$, Where (a) is the lattice parameter, (M) is the

molecular weight, and (N_A) is Avogadro's number. The crystal lattice's uniformity and compactness are reflected in the computed X-ray density of 5.15 g/cm³. Because the ionic radii of the Mg^{2+} ions in the Cu^{2+} differ. This suggests that cationic substitution and strain within the crystal lattice were successful[19]. The produced nano ferrite appears to have a dense and homogeneous structure based on its smaller crystallite size and increased X-ray density.

3.2 FTIR spectrum of $Mg_{0.5}Cu_{0.5}Sm_{0.25}Fe_{1.75}O_4$ nanoferrites

As seen in the **Fig.3** the $Mg_{0.5}Cu_{0.5}Sm_{0.25}Fe_{1.75}O_4$ nano ferrites' Fourier transform infrared spectrum offers important insights into the metal-oxygen vibrations and chemical bonding inside the spinel structure. Two noticeable absorption bands that are typical of spinel ferrites are visible in the spectra; they are situated approximately around 580 cm^{-1} and 400 cm^{-1}. The intrinsic stretching vibration of metal–oxygen (Fe–O) bonds at the tetrahedral (A) sites is responsible for the strong absorption band near 500 cm^{-1}, whereas the vibration of metal–oxygen (Fe–O) bonds at the octahedral (B) sites is responsible for the weaker band seen near 430 cm^{-1}. The development of a separate spinel structure in the Mg-Cu-Sm nano ferrite system is confirmed by these two different vibrational modes[20,21].

Because the bond lengths and force constants at the tetrahedral and octahedral sites differ, these two bands have different positions and intensities. While the lower frequency band at 430 cm^{-1} suggests comparatively poorer metal–oxygen interaction at the octahedral site, the higher frequency band at 580 cm^{-1} indicates better bonding at the tetrahedral site. These distinctive absorption peaks amply demonstrate that $Mg_{0.5}Cu_{0.5}Sm_{0.25}Fe_{1.75}O_4$ ferrite was successfully formed, with mixed metal cations dispersed throughout both lattice locations. Other than these primary peaks, small broad features in the upper wavenumber area (about 3400 cm^{-1} and 1600 cm^{-1}, if present) might be O–H stretching and bending vibrations brought on by residual hydroxyl groups on the particle surface or adsorbed water[22,23]. The synthesized sample's phase purity is indicated by the lack of additional impurity bands.

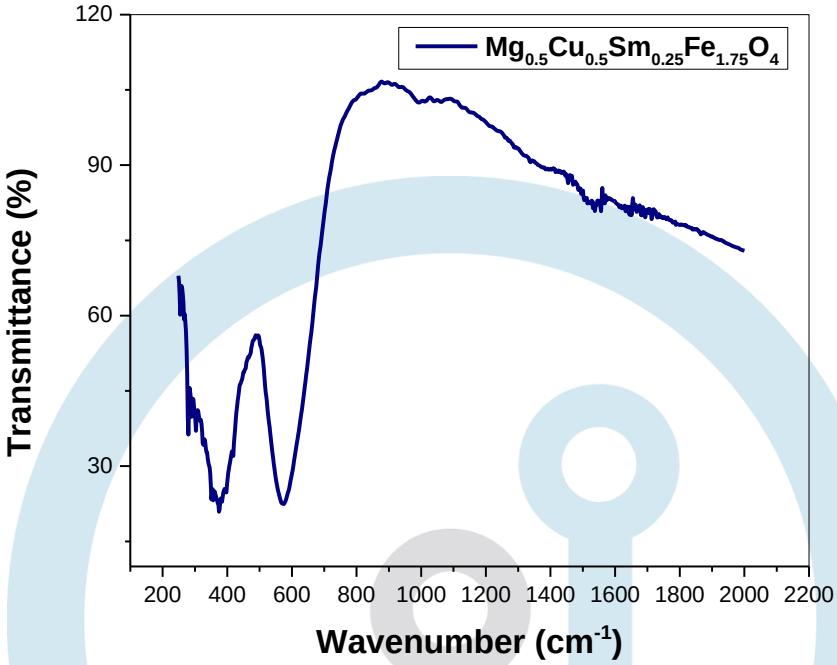

Fig.3 FTIR spectrum of $Mg_{0.5}Cu_{0.5}Sm_{0.25}Fe_{1.75}O_4$ nano ferrites

3.3 Raman spectrum of $Mg_{0.5}Cu_{0.5}Sm_{0.25}Fe_{1.75}O_4$ nanoferrites

The **Fig.4 (a & b)** depicting the Raman spectrum of $Mg_{0.5}Cu_{0.5}Sm_{0.25}Fe_{1.75}O_4$ nano ferrites, offers vital details about the cation distribution, structural order, and vibrational properties of the spinel ferrite lattice. Raman spectroscopy is a useful technique for examining the short-range order in nanocrystalline materials because of its high sensitivity to local symmetry and lattice vibrations. The current spectrum shows a number of different Raman active modes in the 100–800 cm^{-1} wavenumber range, which are typical of ferrites of the spinel type that are part of the Fd3m space group[24,25]. The experimental data is represented by the red curve, and the deconvoluted individual vibrational modes that contribute to the overall spectrum are indicated by the green colour curves.

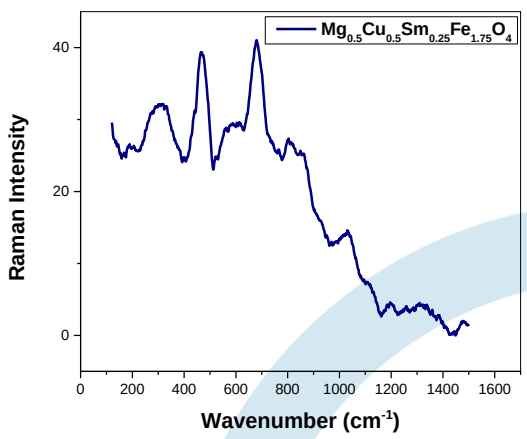

Fig.4 (a) Raman spectrum of $Mg_{0.5}Cu_{0.5}Sm_{0.25}Fe_{1.75}O_4$ nano ferrites

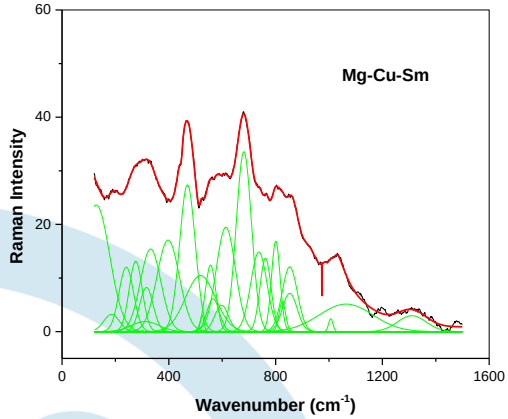

Fig.4 (b) Raman deconvoluted spectrum of $Mg_{0.5}Cu_{0.5}Sm_{0.25}Fe_{1.75}O_4$ nano ferrites

The significant Raman peaks at around 677 cm^{-1}, 610 cm^{-1}, 442 cm^{-1}, 370 cm^{-1}, 310 cm^{-1}, and 220 cm^{-1} are associated with the A_{1g}, Eg, and T_{2g} modes, which are the typical active modes of cubic spinel ferrites. The A_{1g} symmetric stretching vibration of oxygen atoms at the tetrahedral (A) sites, which is mostly linked to Fe^{3+}-O^{2-} interactions, is responsible for the strongest peak, which is located between 690 and 700 cm^{-1}. The T_{2g} (3) and T_{2g} (1) modes, which include asymmetric stretching and bending vibrations of metal–oxygen bonds at both tetrahedral and octahedral sites, are responsible for the bands seen at about 442 cm^{-1} and 610 cm^{-1}, respectively. The octahedral (B) sites' lattice vibrations and translational modes involving cations are represented by the weaker peaks at lower frequency (200–400 cm^{-1}). The coexistence of Mg^{2+}, Cu^{2+} and Sm^{3+} ions at various lattice sites is shown by the appearance of numerous overlapping peaks in the deconvoluted spectra. This causes local distortion and cation redistribution inside the spinel lattice. The inclusion of bigger Sm^{3+} ions instead of smaller Fe^{2+} ions cause lattice expansion and decreased bond strength, which is why the Additionally, the Raman peaks' intensity and broadness show partial disorder and strain in the spinel lattice, which are frequently seen in nanostructured ferrites as a result of surface effects and smaller particle sizes.

3.4 Hysteresis loops of $Mg_{0.5}Cu_{0.5}Sm_{0.25}Fe_{1.75}O_4$ nanoferrites

The Vibrating Sample Magnetometer (VSM) examination of $Mg_{0.5}Cu_{0.5}Sm_{0.25}Fe_{1.75}O_4$ nano ferrites revealed a magnetic hysteresis loop that displays normal ferromagnetic activity, as illustrated in the **Fig.5**. A strong magnetic response with moderate coercivity and clearly defined saturation magnetization is shown by the S-shaped loop[26,27]. The material appears to have substantial magnetic ordering because of the efficient exchange interaction between Fe^{2+} ions at tetrahedral (A) and octahedral (B) sites, as indicated by the saturation magnetization (Ms) value of 27.78 emu/g. In comparison to pure spinel ferrites, weak magnetic Sm^{3+} ions tend to dilute the magnetic exchange interaction and decrease the total magnetization, as indicated by the moderate value of Ms.

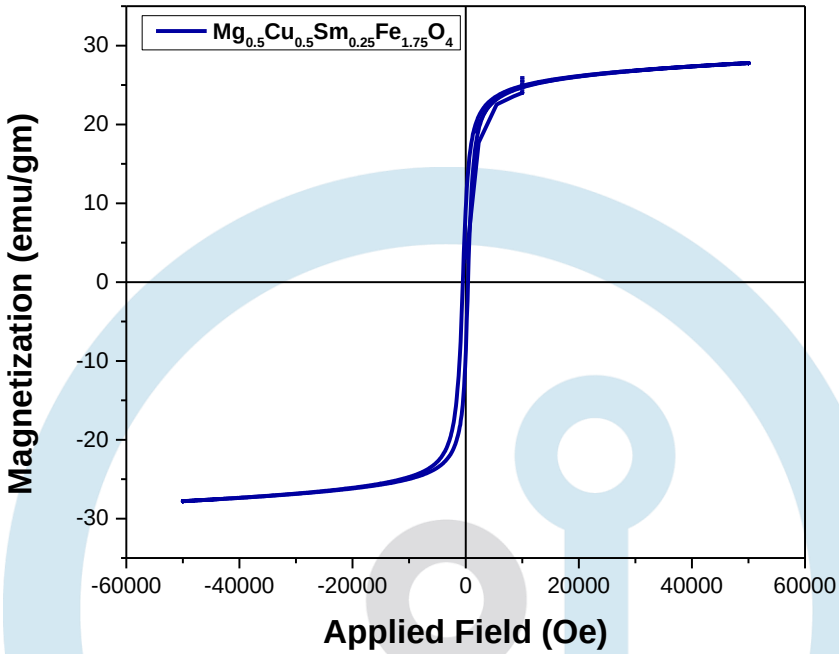

Fig.5 Hysteresis loops of $Mg_{0.5}Cu_{0.5}Sm_{0.25}Fe_{1.75}O_4$ nano ferrites

Since the sample's coercivity (Hc) value is approximately 417.33 Oe, it can be classified as a soft magnetic material. The material is appropriate for high-frequency and transformer core applications because to its low coercivity, which suggests that the magnetic domains can readily realign with an applied magnetic field. After the external field is removed, the remanence magnetization (Mr), which is 19.60 emu/g, indicates that the magnetic domains are somewhat aligned. Single-domain or virtually single-domain behaviour is indicated by the Mr/Ms ratio of 0.705, which points to tiny particle sizes in the nanometer range. The sample's superparamagnetic-like propensity, which is frequently observed in nano ferrites because of surface spin canting and smaller particle sizes, is further supported by the tiny hysteresis loop. The cation distribution between A and B sites in the spinel lattice controls the reported magnetic properties.

4. Conclusions

$Mg_{0.5}Cu_{0.5}Sm_{0.25}Fe_{1.75}O_4$ nano ferrites were successfully synthesized using the citrate-gel auto-combustion method, confirming a single-phase cubic spinel structure with good crystallinity. XRD analysis revealed a crystallite size of 28.69 nm and a lattice parameter of 7.89 Å, indicating proper cation substitution and homogeneous formation. FTIR and Raman studies verified the presence of characteristic metal–oxygen vibrations and Raman-active modes corresponding to tetrahedral and octahedral sites, confirming structural integrity and cation distribution. The VSM analysis showed a soft ferromagnetic nature with a saturation magnetization of 27.78 emu/g, coercivity of 417.33 Oe, and remanence of 19.60 emu/g, suitable for high-frequency and transformer core applications. The moderate magnetization and low coercivity reflect the influence of Sm^{3+} substitution on exchange interactions. Overall, the structural, vibrational, and magnetic results demonstrate that the synthesized Mg–Cu–Sm nano ferrites possess excellent homogeneity, nanocrystalline nature, and desirable soft magnetic characteristics for advanced electronic application.

Acknowledgement

Authors are thankful to department of Chemistry, MVS Govt. Arts and Science College, Mahabubnagar, Telangana, India.509001.

References

[1] B. Yalcin, Exploration of the potential of Co/Cu co-doped Fe2O4 for medical applications: nanostructure, catalytic properties, and blood compatibility, Journal of Nanoparticle Research 24 (2022). https://doi.org/10.1007/s11051-022-05645-7.

[2] M. Satalkar, S.N. Kane, T. Tatarchuk, J.P. Araújo, Ni addition induced changes in structural, magnetic, and cationic distribution of Zn0.75−xNixMg0.15 Cu0.1Fe2O4 nano-ferrite, in: Springer Proceedings in Physics, 2018. https://doi.org/10.1007/978-3-319-92567-7_23.

[3] S. Badr, S.A. Saafan, L.I. Soliman, M.K. El-Nimr, A.A. Kamal, A. El-razek Mahmoud, M. El-Tahawy, Investigation of BaTiO3/ Cu1-xMgxFe2O4 nano-multiferroic composites, J Magn Magn Mater 590 (2024). https://doi.org/10.1016/j.jmmm.2023.171690.

[4] D. Parajuli, P. Taddesse, N. Murali, K. Samatha, Correlation between the structural, magnetic, and dc resistivity properties of Co0.5M0.5-xCuxFe2O4 (M = Mg, and Zn) nano ferrites, Appl Phys A Mater Sci Process 128 (2022). https://doi.org/10.1007/s00339-021-05211-3.

[5] D. Parajuli, N. Murali, A.V. Rao, A. Ramakrishna, Y.M. S, K. Samatha, Structural, dc electrical resistivity and magnetic investigation of Mg, Ni, and Zn substituted Co-Cu nano spinel ferrites, S Afr J Chem Eng 42 (2022). https://doi.org/10.1016/j.sajce.2022.07.009.

[6] H. Khedri, A. Gholizadeh, Experimental comparison of structural, magnetic and elastic properties of M0.3Cu0.2Zn0.5Fe2O4 (M = Cu, Mn, Fe, Co, Ni, Mg) nanoparticles, Appl Phys A Mater Sci Process 125 (2019). https://doi.org/10.1007/s00339-019-3010-1.

[7] V. Ludhiya, N.H. kumar, A. Edukondalu, D. Ravinder, Solution combustion synthesis of nanostructured Mg0.5Ni0.3Cu0.2CexFe2-xO4 ferrites: structural, optical and electromagnetic properties, Appl Phys A Mater Sci Process 129 (2023). https://doi.org/10.1007/s00339-023-06906-5.

[8] A. Hajalilou, M. Hashim, R. Ebrahimi-Kahrizsangi, H. Mohamed Kamari, N. Sarami, Synthesis and structural characterization of nano-sized nickel ferrite obtained by mechanochemical process, Ceram Int 40 (2014). https://doi.org/10.1016/j.ceramint.2013.11.032.

[9] V. Naidu, S.K.A.A. KanduSahib, A. M.SheikDawood, A. M.Suganthi, "Magnetic Properties of Nano Crystalline Nickel, Samariumdoped Zinc Ferrite," Int J Comput Appl 24 (2011). https://doi.org/10.5120/2923-3862.

[10] D.R. Kumar, S.I. Ahmad, C.A. Lincoln, D. Ravinder, Structural, optical, room-temperature and low-temperature magnetic properties of Mg–Zn nanoferrite ceramics, Journal of Asian Ceramic Societies 7 (2019) 53–68. https://doi.org/10.1080/21870764.2018.1563036.

[11] D.R. Kumar, C.A. Lincoln, D. Ravinder, S.I. Ahmad, Structural, morphological, luminescence, magnetic, and electrical transport properties of zinc-doped MnFe2O4 nanomaterials, Appl Phys A Mater Sci Process 126 (2020). https://doi.org/10.1007/s00339-020-03894-8.

[12] I. Shakir, A. Rasheed, S. Haider, M.F. Aly Aboud, The Impact of Cu2+ and Mg2+ onto the electrochemical energy storage properties of Nanocrystalline Co0.8Ni0.2Fe2O4 particles and their hybrids with graphene, Ceram Int 45 (2019). https://doi.org/10.1016/j.ceramint.2019.05.066.

[13] I. Salma, M. Ajaz-un-Nabi, J. Yasir, A. Nasir, Synthesis of Mn 1-x Zn x Fe 2 O 4 ferrite powder by co-precipitation method, IOP Conf Ser Mater Sci Eng 60 (2014).

[14] S.N. Kane, M. Satalkar, Correlation between magnetic properties and cationic distribution of Zn0.85−xNixMg0.05Cu0.1Fe2O4 nano spinel ferrite: effect of Ni doping, J Mater Sci 52 (2017). https://doi.org/10.1007/s10853-016-0636-7.

[15] S. Irfan, M. Ajaz-Un-Nabi, Y. Jamil, N. Amin, Synthesis of Mn1-xZnxFe2O4 ferrite powder by co-precipitation method, in: IOP Conf Ser Mater Sci Eng, 2014. https://doi.org/10.1088/1757-899X/60/1/012048.

[16] M.A. Ansari, S. Akhtar, M.A. Rauf, M.N. Alomary, S. Alyahya, S. Alghamdi, M.A. Almessiere, A. Baykal, F. Khan, S.F. Adil, M. Khan, M.R. Hatshan, Sol–gel synthesis of dy-substituted ni0.4cu0.2zn0.4 (fe2-xdyx)o4 nano spinel ferrites and evaluation of their antibacterial, antifungal, antibiofilm and anticancer potentialities for biomedical application, Int J Nanomedicine 16 (2021). https://doi.org/10.2147/IJN.S316471.

[17] G.K. Salman, A.J. Bohan, G.M. Jaed, Use of Nano-Magnetic Material for Removal of Heavy Metals from Wastewater, Engineering and Technology Journal 35 (2017). https://doi.org/10.30684/etj.35.9a.6.

[18] M.I. Arshad, S. Arshad, K. Mahmood, A. Ali, N. Amin, Umaid-ur-Rehman, M. Isa, A. Akram, N. Sabir, M. Ajaz-un-Nabi, Impact of Mg doping on structural, spectral and dielectric properties of Cd–Cu nano ferrites prepared via sol-gel auto combustion method, Physica B Condens Matter 599 (2020). https://doi.org/10.1016/j.physb.2020.412496.

[19] B. Chethan, H.G. Raj Prakash, S.C. Vijayakumari, Y.T. Ravikiran, Structural and electrical properties of nickel substituted cadmium ferrite, in: AIP Conf Proc, 2018. https://doi.org/10.1063/1.5032875.

[20] D. Ravi Kumar, C.A. Lincoln, G. Vijaya Charan, G. Thara, D. Ravinder, M. Veeraswamy, P. Naresh, Study of photo catalytical, antimicrobial activity, dielectric and ac impedance properties of Zn doped Mg nanoferrites synthesized from citrate gel auto combustion method, Mater Chem Phys 278 (2022). https://doi.org/10.1016/j.matchemphys.2021.125648.

[21] M. Hashim, D. Ravvinder Nayak, A. Ahmed, S. Kumar, S.E. Shirsath, M.M. Ismail, S.K. Sharma, M.A. Alayasreh, R. Kumar, D. Ravinder, R.B. Jotania, S.S. Meena, K.M. Batoo, Structural, dielectric, electric and magnetic properties of magnesium substituted lithium nanoferrites, Ceram Int 49 (2023). https://doi.org/10.1016/j.ceramint.2023.07.056.

[22] P. Shanthakumari, N.H. kumar, A. Edukondalu, D. Ravinder, Effect of neodymium doping on structural, optical, and dielectric properties of Ni ferrites synthesized by citrate gel auto-combustion method, Journal of Materials Science: Materials in Electronics 34 (2023) 1775. https://doi.org/10.1007/s10854-023-11193-0.

[23] L. Phor, S. Chahal, V. Kumar, Zn2+ substituted superparamagnetic MgFe2O4 spinel-ferrites: Investigations on structural and spin-interactions, Journal of Advanced Ceramics 9 (2020) 576–587. https://doi.org/10.1007/s40145-020-0396-3.

[24] S.N. Pund, P.A. Nagwade, A. V. Nagawade, A. V. Bagade, Influence of Cu2+ substitution on structural and optical properties of Mg-Zn ferrite nanoparticles, Mater Today Proc 49 (2022) 2382–2391. https://doi.org/10.1016/J.MATPR.2021.09.402.

[25] P.N. Patil, S. Kumar, A. Anshu, V.M. Jali, B. Sahoo, Green synthesis of meso-porous CuFe2O4 nanoparticles through aloe-vera assisted sol–gel auto-combustion method, Journal of Materials Science: Materials in Electronics 36 (2025) 825. https://doi.org/10.1007/s10854-025-14930-9.

[26] S. Goud, N. Venkatesh, D.R. Kumar, D. Ayodhya, P. Veerasomaiah, Impact of Sm doping on structural, optical, photocatalytic, anti-microbial and electromagnetic properties of Cu-Zn nanoferrites by citrate-gel auto combustion method, J Mol Struct 1310 (2024) 138241. https://doi.org/10.1016/j.molstruc.2024.138241.

[27] A.K. Ambala, N. Venkatesh, C. Jyothirmai, D.R. Kumar, Ch.A. Lincoln, Investigation of structural morphological optical and magnetic properties of Mg-Ce nano ferrites prepared by citrate gel auto combustion method, in: 2025: p. 030009. https://doi.org/10.1063/5.0299122.